Journal of Materials Chemistry A

PAPER

View Article Online
View Journal | View Issue

Cite this: J. Mater. Chem. A, 2015, 3, 23829

Lead-free germanium iodide perovskite materials for photovoltaic applications†

Thirumal Krishnamoorthy,‡[a] Hong Ding,‡[b] Chen Yan,‡[ac] Wei Lin Leong,[d] Tom Baikie,[a] Ziyi Zhang,[b] Matthew Sherburne,[b] Shuzhou Li,[c] Mark Asta,*[b] Nripan Mathews*[acd] and Subodh G. Mhaisalkar[ac]

Received 26th July 2015
Accepted 12th October 2015

DOI: 10.1039/c5ta05741h

www.rsc.org/MaterialsA

Computational screening based on density-functional-theory calculations reveals Ge as a candidate element for replacing Pb in halide perovskite compounds suitable for light harvesting. Experimentally, three $AGeI_3$ (A = Cs, CH_3NH_3 or $HC(NH_2)_2$) halide perovskite materials have been synthesized. These compounds are stable up to 150 °C, and have bandgaps correlated with the A-site cation size. $CsGeI_3$-based solar cells display higher photocurrents, of about 6 mA cm^{-2}, but are limited by poor film forming abilities and oxidising tendencies. The present results demonstrate the utility of combining computational screening and experimental efforts to develop lead-free halide perovskite compounds for photovoltaic applications.

Following up on the initial synthesis of $CsPbX_3$ (X = Cl, Br or I) perovskites, Weber *et al.* successfully replaced Cs^+ with methylammonium ($CH_3NH_3^+$) cations, opening up a new horizon for the development of inorganic–organic metal-halide perovskite materials.[1] In the past decade, major breakthroughs have come with this series of materials in photovoltaic applications, leading to a rapid increase in interest in these materials.[2–4] Since 2009, the power conversion efficiency of devices based on inorganic–organic perovskites has leapt from 3.8% to the most recent highest certificated value of 20.1%.[5–7] This value has surpassed the efficiencies of devices based on amorphous silicon and is almost on par with those using CdTe or CIGS. With such promising device efficiency, low cost of starting materials and simple solution processing, organic–inorganic halide perovskites are an attractive alternative to conventional photovoltaics. One key concern for the future large-scale manufacturing and commercialization of current perovskite-based photovoltaic devices is that they may release Pb into the environment. For example, in a scenario of solar cell encapsulation rupture, Pb ions may dissolve into rainwater causing significant environmental impact. In this context, future commercial utilization requires the replacement of Pb in the perovskite structure, while maintaining analogous optical and photovoltaic performance.[8,9]

In the present work, high-throughput computational methods based on density-functional theory (DFT) were used to screen for candidate inorganic halide perovskites AMX_3, with desirable bandgaps and chemical stability. A total of 360 AMX_3 chemical compositions were considered, with A^{1+} and X^{1-} ions chosen from {K, Rb and Cs} alkali metals and {Cl, Br and I} halogen elements, respectively, in combination with 40 candidate divalent M-site cations. First-principles calculations were performed within the framework of DFT employing the projector augmented wave method and the Perdew–Burke–Ernzerhof (PBE) generalized gradient approximation for the exchange–correlation energy, as implemented in the Vienna *ab initio* simulation package.[10–13] The computed PBE bandgaps (E_g^{PBE}) are illustrated in Fig. 1. Although the bandgaps predicted from PBE-DFT calculations are expected to underestimate the true values measured experimentally, the computational screening exercise uses the values of E_g^{PBE} to explore overall trends across the different chemistries. Further, we note that our team has successfully fabricated $CsSnI_3$ perovskite solar cells and achieved high photocurrent densities under simulated full sunlight. The experimentally measured bandgap of $CsSnI_3$ was 1.3 eV,[14,15] while the calculated value is E_g^{PBE} = 0.44 eV for cubic $CsSnI_3$. We thus use this compound as a calibration point for our calculations, and search for other AMX_3 chemical compositions with E_g^{PBE} in the range of 0.2–0.7 eV. From the results of the computational screening exercise, considering only the calculated bandgap values, we identified 9 candidate compositions: $KSnBr_3$, $KSnI_3$, $RbSnBr_3$, $RbSnI_3$, $CsSnBr_3$, $KGeBr_3$, $KGeI_3$, $RbGeI_3$ and $CsGeI_3$. The thermodynamic

[a]Energy Research Institute @ NTU(ERI@N), Research Techno Plaza, X-Frontier Block, Level 5, 50 Nanyang Drive, 637553, Singapore. E-mail: Nripan@ntu.edu.sg
[b]Department of Materials Science and Engineering, University of California, Berkeley, CA 94720, USA. E-mail: mdasta@berkeley.edu
[c]School of Materials Science and Engineering, Nanyang Technological University, Nanyang Avenue, 639798, Singapore
[d]Institute of Materials Research and Engineering (IMRE), Agency for Science, Technology and Research (A*STAR), 3 Research Link, Singapore 117602, Singapore

† Electronic supplementary information (ESI) available. See DOI: 10.1039/c5ta05741h

‡ These authors contributed equally to this work.

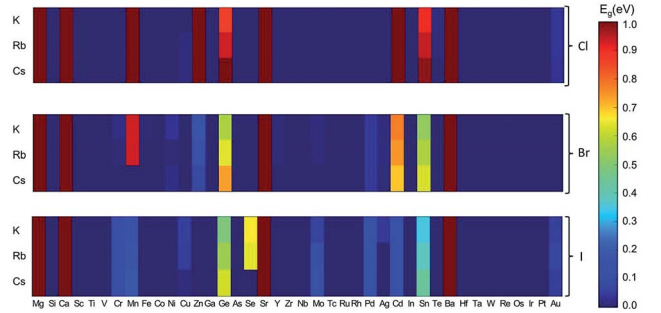

Fig. 1 Predicted PBE functional bandgaps of the 360 AMX_3 halide perovskite compositions. The top, middle and bottom section correspond to X-site species with halogens X = Cl, Br and I, respectively, and in each session, the *x* and *y* axes correspond to M- and A-site components.

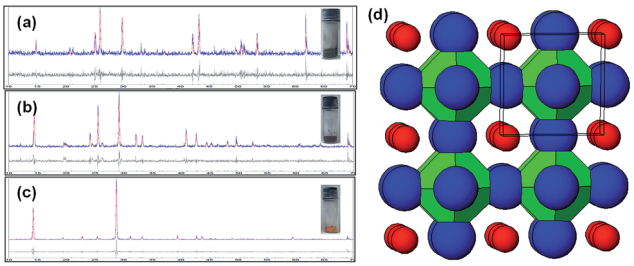

Fig. 2 Pawley fit of the powder X-ray diffraction patterns of (a) $CsGeI_3$, (b) $MAGeI_3$ and (c) $FAGeI_3$ confirming single-phase samples adopting the rhombohedral symmetry (*R*3*m*) at room temperature. (d) Crystal structure adopted by the $AGeI_3$ perovskite.

stability of these compositions was further evaluated through the Materials Project database[16] with calculated energies to determine whether the AMX_3 compositions would decompose to simpler binary phases. We found that only three of the candidate compositions, namely $RbSnBr_3$, $CsSnBr_3$ and $CsGeI_3$, are predicted to be energetically stable (as shown in Table S1†).

Due to the significant underestimation of bandgaps by the PBE method, we repeated the computational screening exercise described in the previous paragraph employing the Δ-sol approach,[23] which features comparable computational cost to PBE, but with improved accuracy for bandgap prediction. Specifically, we calculated by the Δ-sol method the bandgaps of compounds for which $E_g^{PBE} > 0.1$ eV, identifying all with calculated values within 20% of that for $CsSnI_3$. Of these, the compounds that were predicted to be energetically stable were the same as those identified from the PBE-based calculations described above, namely $RbSnBr_3$, $CsSnBr_3$ and $CsGeI_3$.

Sn-based perovskites have been considered in the literature to a much greater degree than Ge-based halide perovskites. Hence, in subsequent experimental work we focussed attention on the potential applications of Ge-based halide perovskite compounds for solar cells.

Experimentally, we have synthesized both the inorganic germanium halide perovskite ($CsGeI_3$), as well as alternative hybrid perovskites where the A^+ cation is replaced with methylammonium (MA) and formamidinium (FA) molecules (see ESI† for the detailed procedure). Fig. 2(a)–(c) show the X-ray diffraction characterization of the three different synthesized samples which can all be indexed to trigonal cells (with a *R*3*m* space group symmetry), in good agreement with previous reports.[17,18] Extracted lattice parameters of rhombohedral unit cells can be seen in Fig. S3.† We note that the room temperature $CsGeI_3$ rhombohedral crystal structure (a = 5.98 Å and α = 88.6°), is very close to the cubic perovskite structure considered in the calculations (a = 5.99 Å and α = 90°). The replacement of Cs with larger MA or FA molecules leads to a rhombohedral angle (α) that is further away from 90°. The increased structural distortions due to cation replacement are also consistent with the prediction based on empirical perovskite tolerance factors which shows a larger deviation from one with a larger A-site cation. Many of the halide perovskites exhibit multiple phase transitions at temperature ranges achievable by a solar cell under external operating conditions. Such structural phase transitions are expected to influence the electronic band structure of the material and therefore impact the photovoltaic properties. The long-term stability of the device may also have an effect because of the change in volume of the crystal.[19] In contrast, variable temperature XRD measurements in the germanium halides reveal no structural change to a higher symmetry cubic system for any of the Ge samples investigated (as shown in Fig. S3†). For each perovskite, an increase in temperature resulted in a corresponding increase in the angle α towards 90°, however complete sample decomposition was observed before a 90° angle, and hence a cubic system could not be obtained. Although the perovskite tolerance factor can be a useful guide to predict the stability of the perovskite structure-type, it does not take into account distortions arising from electronic contributions, *e.g.* the influence of stereochemically active nS^2 lone-pair electrons that generally become more pronounced through the Pb^{2+}, Sn^{2+} and Ge^{2+} series. In this context, detailed structural investigation is still required to elucidate the symmetry properties of these materials, and will form part of our future work.[18,20]

Fig. S4† shows the TGA curve of all three Ge-based perovskite compounds collected under a nitrogen atmosphere. $CsGeI_3$ shows higher stability (up to around 350 °C) in comparison with the other two hybrid perovskites (up to around 250 °C). $MAGeI_3$ follows a single step degradation pathway. This single step could account for the sublimation of the perovskite, but when the material was heated in a glass Petri dish at around 250 °C (in an inert atmosphere) white fumes were released first, immediately followed by orange fumes. So it is clear that $MAGeI_3$ decomposes first and the decomposed product goes in to the vapour state. Comparatively, $FAGeI_3$ exhibited less stability and follows a two stage degradation pathway where the first weight loss of 44% was consistent with the complete transformation to GeI_2. Differential scanning calorimetric analysis demonstrates the stability of all three perovskite compounds in the range of device working temperatures.

Fig. 3(a) shows the Tauc plot of germanium perovskites. With increasing size of the A^+ cation in the structure, the colors of the compounds change from black to red and then orange for

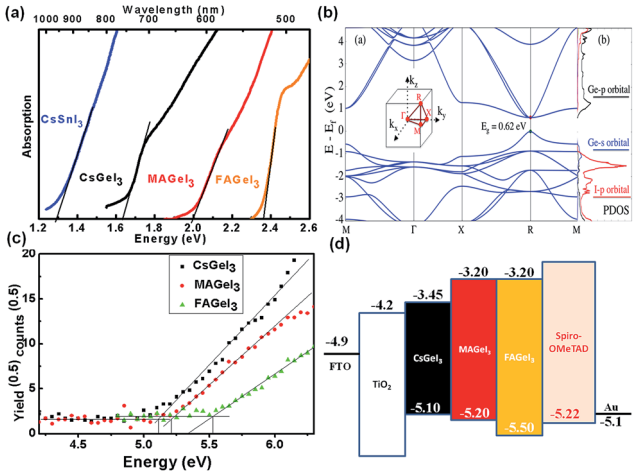

Fig. 3 (a) Optical absorption spectrum of $CsGeI_3$, $MAGeI_3$ and $FAGeI_3$, in comparison with $CsSnI_3$. (b) Calculated band structure and projected density of states of cubic $CsGeI_3$. The energy of the highest occupied state is set to 0 eV. (c) Photoelectron spectroscopy in air (PESA) of powder samples and (b) schematic energy level diagram of $CsGeI_3$, $MAGeI_3$ and $FAGeI_3$.

Cs^+, MA^+ and FA^+ based perovskites. Estimated values of the bandgap derived from Tauc plots are 1.63, 2.0 and 2.35 eV for $CsGeI_3$, $MAGeI_3$ and $FAGeI_3$, respectively. Although the three compounds have bandgaps greater than the ideal one predicted by the Shockley–Queisser limit, $CsGeI_3$ which has a bandgap slightly higher than $CH_3NH_3PbI_3$ could be of great interest. The other larger bandgap perovskites could be good candidates for achieving high open circuit voltage required for making tandem solar cells. The experimentally measured bandgap of $CsGeI_3$ is about 0.4 eV higher than that of $CsSnI_3$, which agrees well with the trends in the calculated PBE bandgaps, as shown in Fig. 1. The computed band structure of cubic $CsGeI_3$, as well as the projected density of states, is plotted in Fig. 3(b). It can be seen that a direct bandgap is located at the *R*-(0.5, 0.5, 0.5) point of the Brillouin zone. The valence band maximum is primarily Ge-s in character, with some hybridization with I-s states, while the character of the states at the conduction band minimum is dominated by Ge-p states. This suggests that the light-absorption would result in an electronic transition that would occur majorly between Ge bonding and antibonding orbitals. This kind of "intra-atomic" band gap structure in general leads to the anomalous bandgap behaviour, where the increase of the lattice constant will give rise to further energy splitting between these orbitals and the corresponding increase in the bandgap of the materials (as noted within these germanium halide perovskites). The bandgap deformation potential $a_g = \mathrm{d}E/\mathrm{dln}\ a$ is calculated as 10.05 eV, which is larger than the values reported for Sn-based perovskites.[21] This suggests the potential for larger bandgap tuning by cation substitution in Ge-based perovskites.

Photoemission spectroscopy in air was used to measure the valence band energy level of all these three Ge-based perovskite compounds and is shown in Fig. 3(c). The measured values of the valence band (VB) of $CsGeI_3$, $MAGeI_3$ and $FAGeI_3$ perovskites are −5.10, −5.2, and −5.5 eV, respectively, and from the observed optical bandgap values, the conduction bands (CBs) are calculated to be −3.47, −3.2 and −3.15 eV, respectively, as shown in Fig. 3(d). The replacement of Cs with MA and FA molecules decreases the valence band level and this follows the same trend as in other metal halide systems.[8,14,22] It must be noted that slight oxidation of the samples during the PESA measurements may have occurred.

We further fabricated solar cells with the germanium iodide perovskites using compact and mesoporous TiO_2 and Spiro-OMeTAD as electron- and hole-selective contacts, respectively. The cross-sectional SEM image of the device architecture is shown in Fig. S5.† However, dissolution of germanium perovskites in most organic polar solvents is not satisfactory due to the presence of hygroscopic phosphorous oxoacids as confirmed by FTIR spectroscopy results (Fig. S6†). Phosphorous acid (added as a reducing agent) with its OH group is involved in hydrogen bonding with iodide, making it very challenging to extract it. Films fabricated with the semi-transparent solutions of perovskites in dimethylformamide (DMF) are shown in Fig. S5.† $CsGeI_3$ and $MAGeI_3$ have a relatively smooth morphology while that of $FAGeI_3$ is very poor. The current density–voltage (*J*–*V*) characteristics of the photovoltaic devices are shown in Fig. 4(a) and Table 1. Our devices exhibit a photocurrent density of 5.7 mA cm^{-2} and 4 mA cm^{-2} for $CsGeI_3$ and $MAGeI_3$ compounds, respectively, as shown in Fig. 4(a). These values are encouragingly higher than that derived from the pristine Sn-based perovskite compounds. However, the solar cells suffered from very poor open circuit voltages. The poor performance of the devices could be attributed to Ge^{4+} formation by oxidation (supported by XPS measurements as shown in Fig. S7 & S8†) during the synthesis and fabrication procedures. The poor solubility of these compounds in polar solvents is an additional limiting factor. Due to the poor film quality of $FAGeI_3$ as shown in Fig. S5,† solar cells did not show any photocurrent. Due to the instability of the $CsGeI_3$ film in ambient atmosphere, only IPCE measurements of the $MAGeI_3$ device were performed (Fig. 4(b)). It can be seen that the device was responsive from about 620 nm and the integrated photocurrent (3.7 mA cm^{-2}) corresponded well with the short circuit current density. Newer preparation methods of Ge-based perovskites without the addition of hypophosphorous acid and under strict control of the synthesis atmosphere, and precursors may lead to significant improvement of the film quality and the corresponding device performance. Another

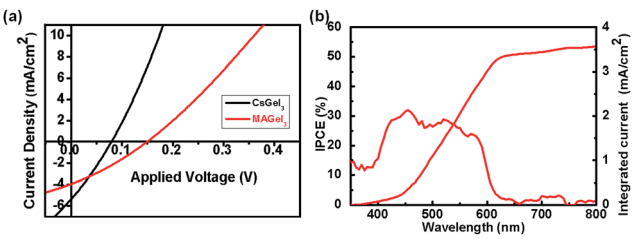

Fig. 4 (a) *J*–*V* curves of photovoltaic devices fabricated with different germanium halide perovskites. (b) IPCE spectrum of the $MAGeI_3$ device.

Table 1 Photovoltaic performance parameters of perovskite solar cells based on $CsGeI_3$ and $MAGeI_3$ materials under a simulated full sunlight of 100 mW cm^{-2}

Device	J_{sc} (mA cm^{-2})	V_{oc} (mV)	FF (%)	PCE (%)
$CsGeI_3$	5.7	74	27	0.11
$MAGeI_3$	4.0	150	30	0.20

possibility is to form the devices through vacuum evaporation, although the challenges of disproportionation also need to be considered. This should be combined with a judicious choice of the HTM to ensure efficient hole extraction.

In summary, computational screening has suggested that germanium may act as a suitable replacement for lead in halide perovskite materials for solar cell applications. Experimentally $CsGeI_3$ crystals with stable rhombohedral crystal structures have been synthesized, which do not show phase changes in the range of device working temperatures. Further, we also synthesized $MAGeI_3$ and $FAGeI_3$ crystals and compared their crystal structure, bandgap, and thermal stability. The solar cells exhibited photocurrent values of 5.7 and 4 mA cm^{-2} for $CsGeI_3$ and $MAGeI_3$, respectively. Overall, the results of the present study demonstrate the strong potential of Ge-based halide perovskite compounds in photovoltaic applications.

Acknowledgements

This work was funded by National Research Foundation (NRF), Singapore (CRP NRF2014NRF-CRP002-036) and the Singapore-Berkeley Research Initiative for Sustainable Energy (SinBeRISE) CREATE programme. We acknowledge Dr Chen Shi and Mr Goh Teck Wee for their help with XPS characterization.

References

1 D. Weber, *Z. Naturforsch.*, 1978, **33**, 1443.
2 N. J. Jeon, J. H. Noh, W. S. Yang, Y. C. Kim, S. Ryu, J. Seo and S. I. Seok, *Nature*, 2015, **517**, 476.
3 T. Krishnamoorthy, F. Kunwu, P. P. Boix, H. Li, T. M. Koh, W. L. Leong, S. Powar, A. Grimsdale, M. Gratzel, N. Mathews and S. G. Mhaisalkar, *J. Mater. Chem. A*, 2014, **2**, 6305.
4 G. Xing, N. Mathews, S. Sun, S. S. Lim, Y. M. Lam, M. Grätzel, S. Mhaisalkar and T. C. Sum, *Science*, 2013, **342**, 344.
5 W. S. Yang, J. H. Noh, N. J. Jeon, Y. C. Kim, S. Ryu, J. Seo and S. I. Seok, *Science*, 2015, 1234–1237.
6 J. Burschka, N. Pellet, S.-J. Moon, R. Humphry-Baker, P. Gao, M. K. Nazeeruddin and M. Gratzel, *Nature*, 2013, **499**, 316.
7 H. S. Kim, C. R. Lee, J. H. Im, K. B. Lee, T. Moehl, A. Marchioro, S. J. Moon, R. Humphry-Baker, J. H. Yum, J. E. Moser, M. Grätzel and N. G. Park, *Sci. Rep.*, 2012, **2**, 591.
8 F. Hao, C. C. Stoumpos, D. H. Cao, R. P. H. Chang and M. G. Kanatzidis, *Nat. Photonics*, 2014, **8**, 489.
9 N. K. Noel, S. D. Stranks, A. Abate, C. Wehrenfennig, S. Guarnera, A.-A. Haghighirad, A. Sadhanala, G. E. Eperon, S. K. Pathak, M. B. Johnston, A. Petrozza, L. M. Herz and H. J. Snaith, *Energy Environ. Sci.*, 2014, **7**, 3061.
10 G. Kresse, *J. Non-Cryst. Solids*, 1995, **193**, 222.
11 J. P. Perdew, K. Burke and M. Ernzerhof, *Phys. Rev. Lett.*, 1996, **77**, 3865.
12 P. E. Blöchl, *Phys. Rev. B: Condens. Matter Mater. Phys.*, 1994, **50**, 17953.
13 G. Kresse and D. Joubert, *Phys. Rev. B: Condens. Matter Mater. Phys.*, 1999, **59**, 1758.
14 M. H. Kumar, S. Dharani, W. L. Leong, P. P. Boix, R. R. Prabhakar, T. Baikie, C. Shi, H. Ding, R. Ramesh, M. Asta, M. Graetzel, S. G. Mhaisalkar and N. Mathews, *Adv. Mater.*, 2014, **26**, 7122.
15 D. Sabba, H. K. Mulmudi, R. R. Prabhakar, T. Krishnamoorthy, T. Baikie, P. P. Boix, S. Mhaisalkar and N. Mathews, *J. Phys. Chem. C*, 2015, **119**, 1763.
16 A. Jain, S. P. Ong, G. Hautier, W. Chen, W. D. Richards, S. Dacek, S. Cholia, D. Gunter, D. Skinner, G. Ceder and K. A. Persson, *APL Mater.*, 2013, **1**, 011002.
17 G. Thiele, H. W. Rotter and K. D. Schmidt, *Z. Anorg. Allg. Chem.*, 1987, **545**, 148.
18 C. C. Stoumpos, L. Fraser, D. J. Clark, Y. S. Kim, S. H. Rhim, A. J. Freeman, J. B. Ketterson, J. I. Jang and M. G. Kanatzidis, *J. Am. Chem. Soc.*, 2015, 6804–6819.
19 A. Binek, F. C. Hanusch, P. Docampo and T. Bein, *J. Phys. Chem. Lett.*, 2015, **6**, 1249.
20 G. Kieslich, S. Sun and A. K. Cheetham, *Chem. Sci.*, 2014, **5**, 4712.
21 L.-y. Huang and W. R. Lambrecht, *Phys. Rev. B: Condens. Matter Mater. Phys.*, 2013, **88**, 165203.
22 T. M. Koh, K. Fu, Y. Fang, S. Chen, T. C. Sum, N. Mathews, S. G. Mhaisalkar, P. P. Boix and T. Baikie, *J. Phys. Chem. C*, 2014, **118**, 16458.
23 M. K. Y. Chan and G. Ceder, *Phys. Rev. Lett.*, 2010, **105**, 196403.

